

# Comparison of Numerical Methods for Obtaining 2-D Impurity Profile in Semiconductor

(반도체 내에서의 2 차원 불순물 분포를 얻기 위한  
수치해법의 비교)

梁 榮 日\*, 慶 宗 旻\*, 吳 亨 哲\*\*

(Yeong Yil Yang, Chong Min Kyung and Hyeong Cheol Oh)

## 要 約

반도체 내에서의 불순물 분포를 구하기 위한 2 차원 확산문제를 푸는 효과적인 수치 해법을 제시하였다. ADI(Alternating Direction Implicit) 방법과 Gauss 소거법의 조합에 의한 수치해법을 사용하므로써 SOR(Successive Over-Relaxation)이나 stone 방법에 비하여 전산기의 메모리 사용량을 증가시키지 않고도 거의 모든 확산 조건에 대하여 CPU시간을 1/3 이하로 줄일 수 있었다. 상대오차의 크기를 0.01% 이내로 하고 1 차원과 2 차원 문제에 대하여, 여러가지 수치해법의 CPU를 비교하였다. 1 차원 계산결과와 실험결과가 잘 일치하였고, 2 차원 계산결과를 1 차원 계산결과와 잘 비교한 결과, 일치함을 알 수 있었다.

## Abstract

An efficient numerical scheme for assessing the two-dimensional diffusion problem for modelling impurity profile in semiconductor is described. A unique combination of ADI (Alternating Direction Implicit) method and Gauss Elimination has resulted in a reduction of CPU time for most diffusion processes by a factor of 3, compared to other iteration schemes such as SOR (Successive Over-Relaxation) or Stone's iterative method without additional storage requirement.

Various numerical schemes were compared for 2-D as well as 1-D diffusion profile in terms of their CPU time while retaining the magnitude of relative error within 0.001%. good agreement between 1-D and 2-D simulation profile as well as between 1-D simulation profile and experiment has been obtained.

## I. Introduction

For the recent five or six years, process simulation has become a very important step in determining the process condition and device design to achieve the specified circuit behaviour, as evidenced by the wide-spread use of the first extensive one-dimensional simulator, SUPREM (1) As the vertical and the lateral device di-

---

\*正會員, 韓國科學技術院 電氣 및 電子工學科  
(Departemnt of Electrical Engineering, KAIST)  
\*\*正會員, 金星半導體株式會社, 慶北龜尾  
(Gold Star Semiconductor Ltd., Gumi, Kyongbuk.)  
接受日字: 1984年 11月 12日

mension shrink to include, in the restricted chip area, as many devices as possible without the loss of electrical performance of the device, one-dimensional process simulation is found out to be insufficient to predict and correct for the basically two- or three-dimensional device behaviour, such as bulk punchthrough, threshold degradation with channel lengths and widths. A number of 2-dimensional process simulators were reported [2,3,4] to compute the accurate 2-D doping profile in the source and drain regions of short-channel MOSFET's and the channel stop diffusion profile in the bird's beak region. The basic process physics and models being adopted in the 1-D process simulator can be reused in the 2-D simulator with no essential variation, and it can be generally said that the only additional effort in developing 2-D simulator is in devising efficient numerical scheme which is fast and does not occupy too much memory space.

For most of the 1-D simulation problems, the direct solution method such as LU decomposition and Gauss Elimination is the obvious choice for obtaining the fast solution, since the number of nodes in the solution domain is generally small ( $\leq 500$ ) and the number of nonzero entry in the system matrix,  $A$  (in  $Ax=b$ ) is, at most, three. Actually, the 1-D simulator, SUPREM, relies on the Gauss Elimination method for solving the resultant set of linear equations.

However, in most of the two-dimensional diffusion problem solver (In this paper, we are mainly concerned with the diffusion aspects among all fabrication steps.), the iterative methods such as Gauss-seidel and SOR (Successive Over-Relaxation) were almost exclusively incorporated, since it is generally thought that the requirement for memory usage in direct solution method is excessive in the conventional five-point differencing scheme for modelling the 2-D diffusion problem.

In this paper, we will describe a two-dimensional simulator, PRECISE (Program for Efficient Calculation of Impurity Shapes using Elimination) which models the 2-D diffusion equation using ADI (Alternating Direction Implicit) scheme and solves the resultant set of linear equations using Gauss Elimination. In ADI model, the concentration values at

three (instead of five) consecutive points either in x-direction or in y-direction have to be considered simultaneously in solving the system equations. Since the number of nonzero elements in each row of matrix  $A$  (in  $Ax=b$ ) is reduced to, at most, three, the direct solution methods become feasible. The LU decomposition method was excluded here since the system matrix varies with each time step ( $\Delta t$ ) due to the updating of diffusivity values each  $\Delta t$ . Section II shows the result of our 1-dimensional diffusion simulator (DIFSIM) compared to the experimental result and SUPREM result. Various combinations of discretization and solution methods, such as FI (Fully Implicit) plus SOR, CN (Crank-Nicolson) plus SOR, and FI plus Gauss Elimination, were compared in terms of the CPU time and accuracy for 1-dimensional diffusion problem. In section III, the numerical scheme employed in PRECISE is explained, and compared with other iterative methods. The results of 2-D simulation were shown in section IV for the case of ion-implantation and thermal diffusion processes of boron and phosphorus.

## II. One-Dimensional Diffusion Problem

### A. 1-dimensional diffusion simulator:

#### DIFSIM

The physical models for diffusion and oxidation process incorporated in the existing 1-D programs<sup>[1]</sup> will not be rediscussed here for simplicity. Fig. 1 and Fig. 2 show the experimental measurement of boron and phosphorus profile obtained by anodize-and-etch method, compared to the simulation result using SUPREM and using DIFSIM (diffusion simulator), a one-dimensional process simulator. Various physical models including vacancy diffusion model, stress effect, OED (Oxidation-Enhanced Diffusion), segregation and moving boundary flux were incorporated in DIFSIM. as can be seen from Fig. 1(a), (b), the boron and phosphorus profiles after the predeposition step are well predicted either by SUPREM or DIFSIM. However, we found a large discrepancy between the experimental data and SUPREM simulation result for the case of

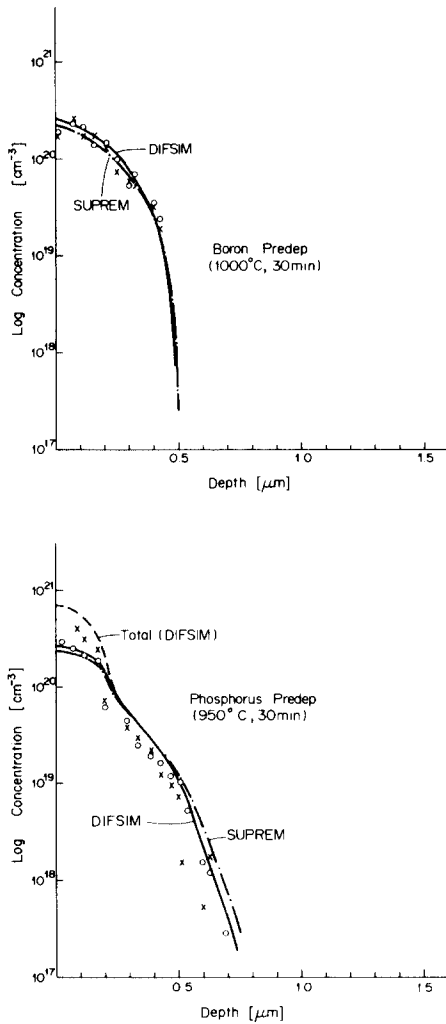


**Fig. 1.** Predeposition profile of (a) boron, and (b) phosphorus by SUPREM, DIFSIM simulation and experiment. 'Total (DIFSIM)' denotes the total concentration of phosphorus as calculated from DIFSIM, while the other two curves denote the electrically active atomic concentrations by DIFSIM and SUPREM. Symbols (o,x) denote two different set of experimental data.

drive-in in oxidizing ambient as is shown in Fig. 2(a) and (b), for boron and phosphorus profile, respectively. The parameter values used in DIFSIM were adjusted to yield the simulation results in good agreement with the experimental data.

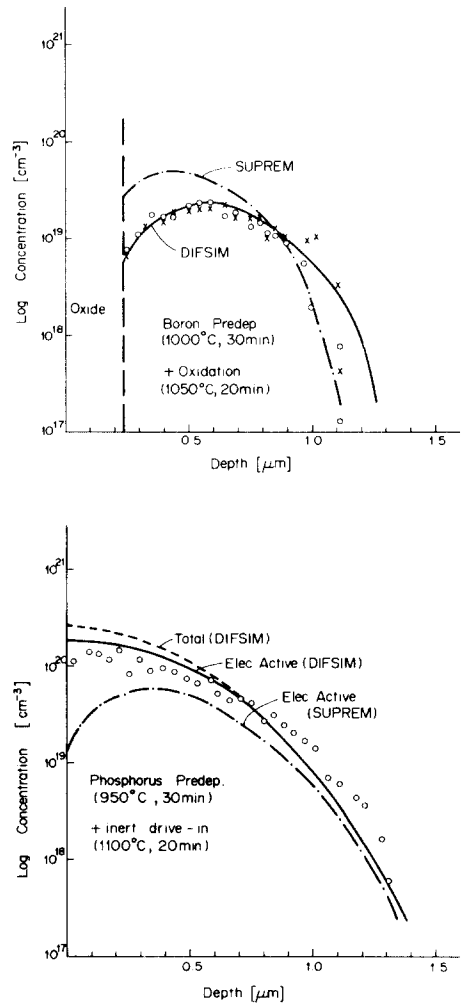


**Fig. 2.** Inert-ambient drive-in profile of (a) boron and, (b) phosphorus by SUPREM DIFSIM simulation and experiment. Symbols (o,x) denote two different set of experimental data.

*B. Comparison of 1-D Numerical Schemes*

The diffusion equation to be solved in semiconductor bulk region, in simplified form, is

$$\frac{\partial C}{\partial t} = \frac{\partial}{\partial x} (D(C) \frac{\partial C}{\partial x}) \tag{Equ. (1)}$$

which can be discretized using various finite difference grid schemes such as implicit method, explicit method, Crank-Nicolson

method and Dufort-Frankel method. The discretizing scheme of each method is summarized in Table 1.

**Table 1.** One-dimensional discretization schemes.

Implicit	$C_j^{n+1} - C_j^n = \alpha(C_{j+1}^{n+1} - 2C_j^{n+1} + C_{j-1}^{n+1})$ $\alpha = D \cdot \Delta t / (\Delta x)^2$
Explicit	$C_j^{n+1} - C_j^n = \alpha(C_{j+1}^n - 2C_j^n + C_{j-1}^n)$
Crank-Nicolson	$C_j^{n+1} - C_j^n = \frac{\alpha}{2} \left[ (C_{j+1}^{n+1} - 2C_j^{n+1} + C_{j-1}^{n+1}) + (C_{j+1}^n - 2C_j^n + C_{j-1}^n) \right]$
Dufort-Frankel	$C_j^{n+1} - C_j^{n-1} = 2\alpha(C_{j+1}^n + C_{j-1}^n - C_j^{n+1})$

Explicit scheme is generally unstable unless excessive care is taken in selecting  $\Delta t$  and, for that reason, has been avoided in most practical applications. DF (Dufort-Frankel method) is a three level time discretization method, and found out to be nonconverging unless the time step ( $\Delta t$ ) is made to be less than 20-30% of that in other methods for the same problem either 1-dimensional or 2-dimensional. For the reason, DF was virtually excluded for comparison in this paper. The discretized equation can be solved either by direct method or iterative method. We have chosen the maximal time step ( $\Delta t$ ) which gives the error in concentration values at every grid point of less than 1% as the optimal  $\Delta t$ . The optimal  $\Delta t$  value was very similar for all the solution methods tried. Fig. 3(a) (b) shows the boron profile after predeposition (950°C, 30 min), where the obviously misleading result appears as  $\Delta t$  jumps from 0.4 min to 0.6 min. Fig. 3(b) shows the case for phosphorus predeposition, where  $\Delta t_{opt}$  was chosen to be 0.1 min. Three different combinations of discretizing schemes and solution methods were compared in Fig. 4 in terms of their CPU time. Case I, II and III denote three different predeposition cycles. The data points represented as filled circles denote FI plus SOR, the open circles denote CN plus SOR, while the X denote FI plus Gauss Elimination.

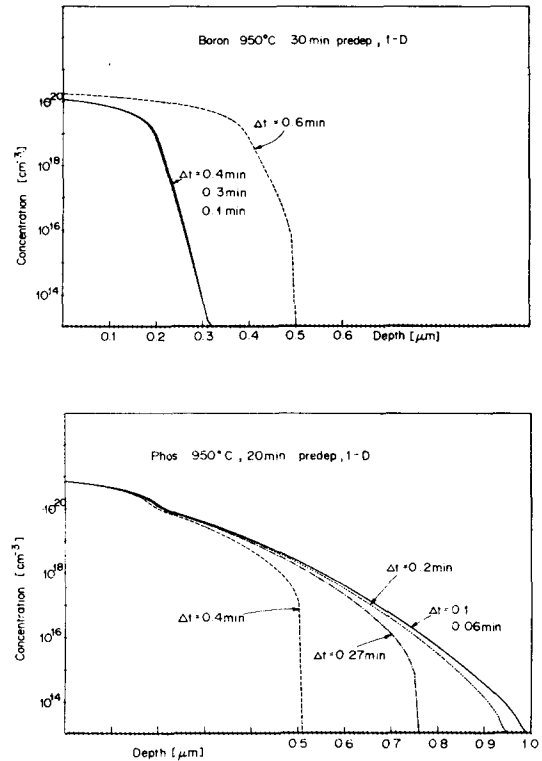


**Fig. 3.** Simulated predeposition profile of (a) boron, and (b) phosphorus using various magnitudes for the time step ( $\Delta t$ ).

Among three cases I, II and III, the phosphorus predep cycle (III) takes longest CPU time due to its highly complicated regional diffusivity behaviour [5]. In any case, however, the FI plus GE scheme has shown a factor of three advantage in CPU time compared to the other two schemes. The time step ( $\Delta t$ ) were refined until 1% error in concentration value occurs. In most cases, the average diffusivity times time step size ( $D_{av} \cdot \Delta t_{opt}$ ) product were nearly constant. Case III shows the smallest  $\Delta t_{opt}$  owing to its relatively high diffusivity value.

### III. Two-Dimensional Diffusion Problem

The two-dimensional diffusion equation

$$\frac{\partial C}{\partial t} = D \left( \frac{\partial^2 C}{\partial x^2} + \frac{\partial^2 C}{\partial y^2} \right)$$

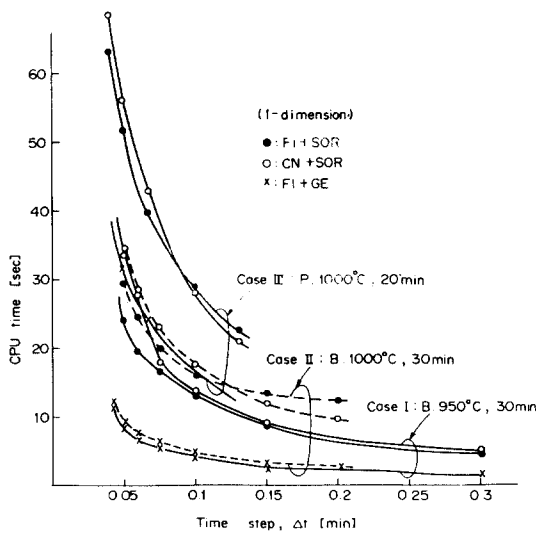


**Fig. 4.** Comparison of CPU times among three numerical methods in three (I, II, and III) cases of one-dimensional predeposition problems. Filled circle denotes Fully-Implicit (FI) plus SOR, empty circle denotes Crank-Nicolson (CN) plus SOR, while x denotes FI plus Gauss Elimination.

can be discretized by the similar schemes as that used in 1-D problem i.e., fully-implicit method, Crank-Nicolson method, etc. In these discretizing schemes, the resultant set of linear equations has been solved by iterative solution methods such as Gauss-Seidel and SOR (Successive Over-Relaxation), or LU decomposition using sparse matrix technique, or Stone's iterative method which updates, at each iteration, the direct solution of the matrix modified to be LU-decomposable.<sup>[6]</sup> In any of the above formulations, the solution procedure is concerned with solving a set of linear equations, where each equation has five unknowns. In this paper, we introduced the ADI (Alternating Direction Implicit) scheme which formulates a two-dimensional problem into a succession of two independent one-dimensional problems as follows.

$$C_{j,k}^{n+1/2} - C_{j,k}^n = \frac{D\Delta t}{2} \cdot \left( \frac{\delta^2 C_{j,k}^{n+1/2}}{\delta x^2} + \frac{\delta^2 C_{j,k}^n}{\delta y^2} \right) \quad \text{Equ. (2)}$$

$$C_{j,k}^{n+1} - C_{j,k}^{n+1/2} = \frac{D\Delta t}{2} \left( \frac{\delta^2 C_{j,k}^{n+1/2}}{\delta x^2} + \frac{\delta^2 C_{j,k}^{n+1}}{\delta y^2} \right) \quad \text{Equ (3)}$$

The above two equations are combined to give

$$C_{j,k}^{n+1} - C_{j,k}^n = D\Delta t \left[ \frac{\delta^2 C_{j,k}^{n+1/2}}{\delta x^2} + \frac{1}{2} \left( \frac{\delta^2 C_{j,k}^n}{\delta y^2} + \frac{\delta^2 C_{j,k}^{n+1}}{\delta y^2} \right) \right] \quad \text{Equ. (4)}$$

A time step ( $\Delta t$ ) is divided into two sub-steps, odd (between  $n$  and  $n+1/2$  in Equ. 2) and even (between  $n+1/2$  and  $n+1$  in Equ. 3) intervals, and the implicit direction (x-direction in Equ. 2, and y-direction in Equ. 3) alternates every  $\frac{\Delta t}{2}$ . The combined form, Equ. 4, is equivalent to treating x-direction by the mid-point rule and the y-direction by the trapezoidal rule like crank-nicolson method. The ADI scheme, when applied to 2 or 3-dimensional diffusion problems were proven to be generally stable<sup>[7]</sup> Since the five-point difference grid scheme has been modified to two three-point difference formulations, we can easily apply the Gauss Elimination method for odd time steps and even time steps. (The node number reordering has to be done each  $\Delta t/2$  to make Gauss Elimination process easy.)

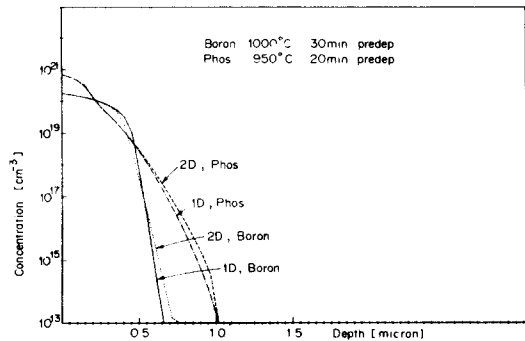


**Fig. 5.** Comparison of 1-D simulation (DIFSIM) and 2-D simulation (PRECISE) for the predeposition of boron and phosphorus.

Fig. 5 shows the comparison of the result of 1-D simulation (DIFSIM) with that of 2-D simulator (PRECISE) for the predeposition cycles of boron and phosphorus. The number of meshes in 2-D simulation was 30x30, while

it was 400 in 1-D simulation. Three different combinations of discretizing and solution methods were compared in terms of the CPU time in Fig. 6(a) and (b) for boron and phosphorus predeposition case, respectively. (A) and (B) denote FI plus stone's iterative method, and FI plus SOR, respectively. Both methods take nearly similar amount of CPU time, while (A) performs better as  $\Delta t$  increases. The average number of iterations at each time step (represented as dotted line) stays fairly constant in the case of boron predeposition (see Fig. 6(a)), while in phosphorus predeposition (Fig. 6(b)), it somewhat increases as  $\Delta t$  increases owing to the highly dependent nature of diffusivity of concentration values. In Fig. 6(a), (b), it is seen that in the method (C), which combines ADI with Gauss Elimination, the CPU time was reduced by approximately a factor of three compared to (A) and (B). (The reduction factor is smaller in phosphorus case due to the CPU time overhead in evaluating the diffusivity.) Method (C) using ADI plus Gauss Elimination was employed in PRECISE for calculating the two-dimensional impurity profile shown in the following section.

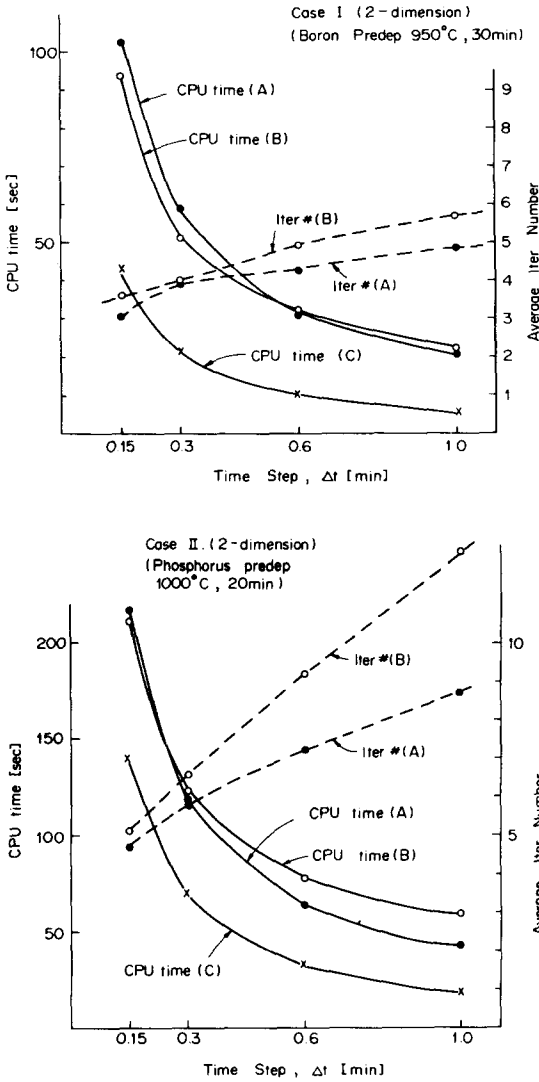


Fig. 6. Comparison of three numerical schemes in 2-D problem for the predeposition of (a) boron, and (b) phosphorus. Method A is FI + stone's method, method B, FI + SOR with  $\omega=1$ , and C is ADI + Gauss Elimination. Left axis quantity is CPU time, while right axis quantity is iteration number averaged over all time steps.

IV. Results and Discussion

Fig. 7 through Fig. 9 show the two-dimensional impurity profile due to ion-implantation, predeposition, and drive-in cycles as obtained

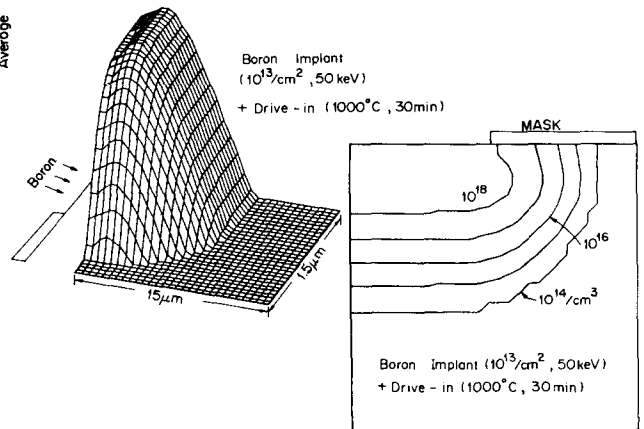


Fig. 7. 2-D profile of boron after the ion implantation ( $10^{13}/50$  KeV) followed by  $1000^{\circ}\text{C}$ , 30 min drive-in.

from PRECISE. The domain size is  $1.5 \mu\text{m} \times$  and divided into  $30 \times 30$  grids. The reflecting boundary conditions were assumed for all boundaries except the mask window for ion-implantation and predeposition. Boron implant profile is assumed to be pearson-IV type distribution in the vertical direction and erfc in the lateral direction. Fig. 7 shows the 2-dimensional boron profile due to ion-implantation ( $10^{13}/\text{cm}^2$  at 50 keV) when half ( $0.75 \mu\text{m}$ ) of the silicon surface was covered with a mask, which was followed by a drive-in cycle of ( $1000^\circ\text{C}$ , 30 min). Implant profile for phosphorus was assumed to be joint-gaussian in the vertical direction and erfc in the lateral dimension. The vertical profile is given as a table-type data, which is the same as that used in SUPREM. Physical models used for the predeposition and drive-in of boron and phosphorus is exactly the same as that used in DIFSIM, and essentially equivalent to that of SUPREM.

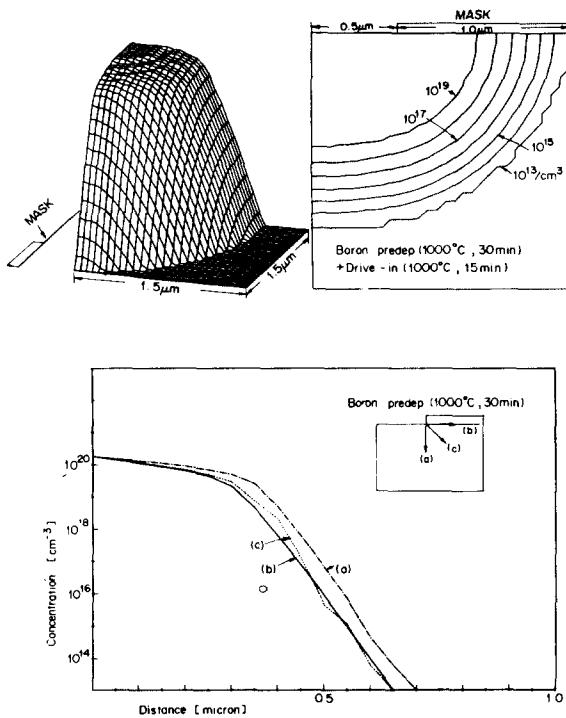


Fig. 8. (a) ; 2-dimensional profile of boron due to predeposition ( $1000^\circ\text{C}$ , 30 min). (b) ; profile in. (c) as seen in three direction from the mask edge.

Fig. 8(a) shows the boron profile following predeposition cycle ( $1000^\circ\text{C}$ , 30 min). In this case the diffusion window is  $0.5 \mu\text{m}$  wide, while the remaining  $1.0 \mu\text{m}$  was covered with a mask. Fig.8(b) shows the same profile in one-dimensional fashion beginning from mask edge in the vertical direction, (a), in the direction along the Si/SiO<sub>2</sub> interface, (b), and  $45^\circ$  direction, (c). Lateral junction depth in  $45^\circ$  direction are shown to be suppressed by a factor of  $0.9 \sim 0.93$ , which can be explained by the relative shortage of impurity source in the corner region. The curve (c) denoting the profile in  $45^\circ$  direction shows some artifact due to inappropriate grid quantizing and interpolation. It is thought that the lateral junction depth will be decreased if the impurity segregation is considered. Fig. 9 shows the boron profile in Fig. 8(a) after the additional thermal cycle (drive-in at  $1000^\circ\text{C}$ , 15 min). It can be seen from Fig. 9 that, following  $1000^\circ\text{C}$ , 30 min predeposition and  $1000^\circ\text{C}$ , 15 min drive-in cycles, the junction depth ( $x_j$ ) due to boron at the center of the mask window begins to shrink from the  $x_j$  value at the center of the mask window which is much wider than the  $x_j$  value.

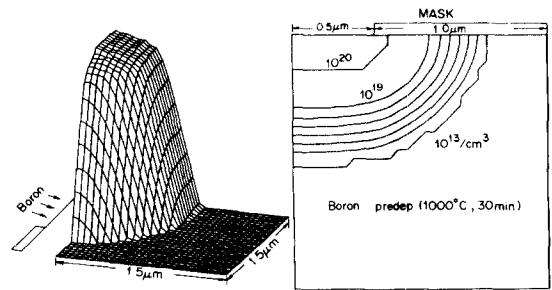


Fig. 9. Profile in Fig. 8 following drive-in ( $1000^\circ\text{C}$ , 15 min).

### V. Conclusion

A two-dimensional numerical scheme combining ADI (Alternating Direction Implicit) with Gauss Elimination was presented. It showed a significant CPU time reduction (about a factor a two or three in our examples) compared to the conventional iterative schemes. Memory requirement is also minimal. The 2-D

program result was calibrated with 1-D program result, which was, in turn, in better agreement with experimental results than SUPREM. Various simulation results, as well as the optimal time step, for implantation, predeposition and drive-in steps of boron and phosphorus were demonstrated.

It is believed that such phenomena as junction depth shortening in the small window region and the anisotropy in diffusion profile due to segregation at the Si/SiO<sub>2</sub> interface in the lateral direction in the mask edge region, can be accurately observed using extensive two-dimensional simulation.

### References

- [1] D.A. Antoniadis and R.W. Dutton, "Models for Computer Simulation of Complete IC Fabrication Processes," *IEEE Trans. Electron Devices*, vol. ED-26, pp. 490, 1979.
- [2] B.R. Penumalli, "Comprehensive Two-Dimensional VLSI Process Simulation Program, BICEPS," *IEEE Trans. Electron Devices*, vol. ED-30, pp. 986, Sept. 1983.
- [3] A. Seidl, "A Multigrid Method for Solution of the Diffusion Equation in VLSI Process Modelling," *IEEE Trans. Electron Devices*, vol. ED-30, pp. 999-1004, Sept. 1983.
- [4] K.A. Salsburg and H.H. Hansen, "FEDSS; Finite-Element Diffusion - Simulation System," *IEEE Trans. Electron Devices*, vol. ED-30, pp. 1004-1011, Sept. 1983.
- [5] R.B. Fair and J.C.C. Tsai, "A Comprehensive Model for the Diffusion of Phosphorus in Silicon and the Emitter Dip Effect," *J. Electrochem. Soc.* pp. 1107-1118, July 1977.
- [6] H.L. Stone, "Iterative Solution of Implicit Approximations of Multi-dimensional Partial Differential Equations," *SIAM J. Numer. Anal.*, vol. 5, pp. 530-558, 1968.
- [7] See Chap. 4, J.H. Ferziger, *Numerical Methods for Engineering Application*. Wiley-Interscience, 1981.